Efficient Iterative Time-Domain Beam Propagation Methods for Ultra Short Pulse Propagation: Analysis and Assessment

Husain M. Masoudi and Mohammad S. Akond

***Abstract*—The time-domain beam propagation method (TD-BPM) has been implemented and analyzed using several iterative numerical techniques to model the propagation of ultra short pulses in optical structures. The methods depend on one-way non-paraxial time domain propagation that use Pade approximant formulation. Several numerical tests showed that the iterative TD-BPM techniques are very stable and converge using few iterations. From accuracy assessment compared to the FDTD, it has been observed that the longitudinal and the temporal steps sizes can be a number of orders of magnitude larger than the FDTD step sizes with little percentage difference. Computer performance analysis showed the TD-BPM is well suited for long dielectric structures interaction of short and ultra short pulse propagation.**

***Index Terms*—beam propagation method, finite-difference analysis, finite-difference time domain, modeling, numerical analysis, optical waveguide theory, Pade approximant, ultra-short pulse propagation.**

I. Introduction

THE rapid progress of ultra-fast nano-optics field for processing and controlling of ultra-fast beam of femtosecond time interaction with nano scale structures has opened new and wide ranges of applications in different fields of science [1], [2]. At the same time, the advancement of interesting and innovative nano photonics materials of photonic crystals, plasmonics and metamaterials are transforming photonics application progressively. At this stage, it is very curtail to develop a collection of accurate and efficient numerical tools for wide applications, especially for short and ultra-short optical pulse interaction.

Most of the numerical techniques available were developed for CW optical applications and very few are appropriate for time domain analysis of ultra-fast domain. The explicit finite difference time domain (FDTD) is probably the most widely used method for both CW and TD applications [3]–[6]. Being an explicit technique, the main drawback of the FDTD is the Courant criterion (CFL) imposed on the time step size. In addition, the spatial step sizes should be much smaller than the wavelength ($\sim\lambda/100$) for proper convergence to small or irrelevant numerical dispersion error. For fine spatial grids, relative to the wavelength to resolve geometrical features of different device levels, even smaller temporal step sizes are required for stability, which increases the computational time many fold. Another restriction for the temporal step size is the Nyquist limit even for continuous wave (CW) analyses [7]. Therefore, the conventional FDTD is not practical for large scale applications [4]. As a result, in the last ten years or so, a family of new FDTD techniques based on implicit approach has been proposed [7]–[14]. The most important two are the alternating direction implicit (ADI-FDTD) [9] and the locally one dimensional (LOD-FDTD) [10] techniques. Being implicit methods, they are free of CFL restriction imposed on the time step size and they showed that they are unconditionally stable. Nevertheless, it was found that their accuracy performances degrade with the increase of the time step size compared to the CFL limit of the explicit FDTD. They also require additional computer resources (memory and CPU time) to handle tri-diagonal matrices at every time update [14]. The envelope versions of the ADI and the LOD depend on the Slowly Varying Envelope (SVE) function extracted from the fields (sometime referred to as Complex Envelope CE FDTD). Although the accuracy of the envelope implicit FDTD are better than the implicit FDTD for large temporal step sizes, but again the accuracy degrades as the time step size increases [14]. More importantly the envelope implicit FDTD produces numerical artifacts of anomalous mode propagation and spurious charges. In fact these artifacts are also present in the implicit FDTD as well [13]. It is to be noted that the CE FDTD is implemented in the complex domain, which adds extra computational demand. Systematic performance evaluation for all the implicit FDTD techniques discussed concluded that their advantages in the optical domain are not clear [14]. On the other hand, both the ADI and the LOD FDTDs are derived from the perturbation of the Crank Nicholson FDTD technique that produces a splitting error proportional to the time step size and the magnitude of the spatial derivatives. Due to this splitting error, these implicit FDTD are suited only for narrowband applications [13]. Furthermore, several implicit techniques have been proposed and tested to solve the time wave equation using Crank-Nicholson (called Full Band—FB), Pade (1,1) approximant (called Wide Band—WB) and the parabolic approximation (called Narrow Band—NB) approaches [15]. It is to be noted that these techniques are also called Time-Domain Beam Propagation Method (TD-BPM), but they use the same mechanism of the FDTD by

Manuscript received March 19, 2011; revised May 23, 2011; accepted June 07, 2011. Date of publication June 16, 2011; date of current version July 29, 2011. This work was supported by King Fahd University of Petroleum and Minerals KFUPM, Dhahran, Saudi Arabia.

The authors are with the Department of Electrical Engineering, King Fahd University of Petroleum and Minerals, Dhahran 31261, Saudi Arabia (e-mail: husainm@kfupm.edu.sa).

Color versions of one or more of the figures in this paper are available online at http://ieeexplore.ieee.org.

Digital Object Identifier 10.1109/JLT.2011.2159703

discretizing the spatial domain and use time stepping mechanism to find the evolution of the field. This is not to be confused with the work presented in here that uses stepping with forward marching along the longitudinal direction z (similar to the classical CW BPM), as will be seen later. Obviously, the NB and the WB are not suited to model short and ultra short pulse propagation due to the approximation involved, and the FB showed that it consumes much larger computer resources as compared to the explicit FDTD in handling a large sparse matrix at every time stepping [15].

A few years back, an efficient unidirectional TD-BPM technique based on the parabolic wave equation, that expanded the wave equation in terms of one-way operator along z while keeping the time variation along with the transverse spatial variations, has been proposed [16], [17]. The operator used direct FD discretization approximation for both time and spatial variations. This arrangement has the advantage of allowing the numerical time window to follow the evolution of the pulse and hence minimizes the computer storage of the problem as well as the execution time. However, this technique showed limitation on handling short and ultra short pulse propagation. The error increases with the decrease of the initial pulsewidth and it was shown that this error is associated with the parabolic approximation. Moreover, a similar operator approach for pulse propagation of ultra short durations in optical structures using non-paraxial wave equation by incorporating the well-known Pade approximants has been proposed and tested [18], [21]. Initial studies for the non-paraxial TD-BPM showed a significant improvement in accuracy as compared to the parabolic technique for ultra short pulse propagation of long device interaction. It is to be noticed that Pade approximant technique has been used effectively in many CW BPM problems for non-paraxial one-way propagation operator and bidirectional BPM problems that involve reflections [22], [23]. In addition, there are a few similar higher-order parabolic equations solutions in non-optical fields such as underwater acoustics and seismology have been reported [22], [24].

In this work, we have implemented and analyzed the non-paraxial TD-BPM using several iterative numerical techniques [19], [20] to model the propagation of ultra short pulse propagation in optical devices for the purpose of enhancing its efficiency. In addition, the method has been tested and compared with the conventional explicit FDTD in terms of convergence and efficiency. We found that the TD-BPM techniques are very stable, accurate and efficient for the propagation of unidirectional ultra short pulse propagation. From accuracy assessment compared to the FDTD, it showed that the longitudinal and the temporal steps sizes can be a number of orders of magnitude larger than the FDTD step sizes with small percentage difference.

II. Formulation

The time domain wave equation for 2-D structures (x and z) can be written as

$$\partial_z(\alpha\,\partial_z\,\Phi)+\partial_x(\alpha\,\partial_x\,\Phi)-\frac{\beta}{c_o^2}\partial_{tt}\Phi=0. \tag{1}$$

The above equation assumes that z is the propagation direction, c_o speed of light in free space and accounts for TE and TM polarizations as: TE (TM) for $\Phi = E_y(H_y)$ with the constants $\alpha = 1(1/n^2)$ and $\beta = n^2(1)$. Upon extracting the carrier frequency of the pulse as $\Phi(x,z,t)=\phi(x,z,t)e^{j(\omega t-n_o k_o z)}$ and also adjusting the movement of the time window with the group velocity v_g of the pulse envelope through the substitution of a moving time coordinate $\tau = t - z/v_g$, changes (1) to [18]

$$\partial_{zz}^2\varphi+\partial_x(\alpha\,\partial_x\,\varphi)=\frac{\beta}{c_o^2}\partial_{\tau\tau}^2\varphi-k_o^2(\beta-\alpha n_o^2)\varphi +2j\left[\alpha n_o k_o\partial_z\varphi+\beta k_o\left(\frac{1}{c_o}-\frac{1}{v_g}\right)\partial_\tau\varphi\right]. \tag{2}$$

Equation (2) can be viewed as a multiplication of two operators, one for forward propagation and the second for backward propagation. For unidirectional pulse propagation, the following can be written for the propagation along the positive z-direction

$$\varphi(x,\Delta z,\tau)=e^{jk_o n_o(1-Q)\Delta z}\varphi(x,z=0,\tau) \tag{3}$$

where $\varphi(x, z = 0,\tau)$ is the initial field and the pseudo-differential operator is defined as

$$Q=\sqrt{L}=\frac{\sqrt{W}}{\sqrt{\alpha}\,n_o\,k_o} \tag{4}$$

where

$$W=\partial_x(\alpha\,\partial_x)-2j\beta k_o\left(\frac{1}{c_o}-\frac{1}{v_g}\right)\partial_\tau -k_o^2(\beta-\alpha n_o^2)\varphi+\frac{\beta}{c_o^2}\partial_{\tau\tau}^2. \tag{5}$$

Pade approximant can be used to approximate the square root exponential operator based on the rational approximation that can be written as [18], [21], [22]

$$e^{-jk_o n_o Q\Delta z}=e^{\rho\sqrt{1+R}}\approx\prod_{i=1}^{m}\frac{1+a_iR}{1+b_iR} \tag{6}$$

where $\rho = -jk_o n_o \Delta\mathrm{z}$ and $R = L - 1$, a and b are called Pade coefficients with m being the Pade order.

III. Numerical Methods

In the above formulation, the finite difference (FD) approximation can be applied to discretize the transverse spatial and the time derivatives of (5) which results in a sparse block tri-diagonal matrix. The diagonal blocks contain tri-diagonal matrices and the off diagonal blocks contain diagonal elements only. The propagation of the pulse along the longitudinal direction requires the operations shown in (6) that needs initially the multiplication of the input field with the numerator of (6) which gives a column vector. The second operation requires the inverse of a large sparse matrix that comes from the denominator operator of the quotient. This process is repeated several times according to the Pade order m that satisfies convergence. There are basically two ways to perform the inversion of the matrix; either using direct algorithm based on the Gaussian elimination technique and its enhancements (referred to in here as direct method) or using iterative algorithms in

TABLE I
ITERATIVE METHODS USED FOR THE TD-BPM AND THEIR AVERAGE NUMBER OF ITERATION FOR CONVERGENCE PER PROPAGATIONAL STEP

Iterative Method	Abbr.	No. of Iterations
BiConjugate Gradients	bicg	4
BiConjugate Gradients Stabilized	bicgstab	2
Conjugate Gradients Squared	cgs	2
Quasi-Minimal Residual	qmr	4
Least Squares	lsqr	3
Minimum Residual	minres	3
Preconditioned Conjugate Gradients	pcg	4
Symmetric LQ	symmlq	3
Generalized Minimum Residual	gmres	4

order to approximate solution using repetitive computation. Iterative methods use a wide range of techniques that employ successive approximations to obtain accurate solutions to a linear system, such as $Ax = b$, at each step [19], [20]. They are particularly useful when the matrix involved A is sparse. In theory, infinite number of iterations might be required to converge to the desired solution. In practice, iteration terminates when the residual $r = ||Ax - b||$, or some other measure of error, is as small as desired. There are several iterative methods such as Jacobi, Gauss-Seidel (GS), Successive Over Relaxation (SOR) and Conjugate Gradient (CG) developed over a period of time for different types of matrices [19], [20]. In each of these methods the matrix needs to be of special type for optimum results. As for example, Jacobi requires strict diagonal dominant elements and its convergence is very slow. GS requires the matrix to be symmetric positive definite. SOR and CG is not directly applicable to non-symmetric or indefinite systems. However, CG can be generalized to non-symmetric systems by sacrificing one of the key features of this method of short recurrence and minimum error. Nevertheless, several generalizations have been developed for solving non-symmetric systems, including Generalized Minimal Residual Method (GMRES), Quasi-Minimal Residual (QMR), Conjugate Gradient Stabilized (CGS), Biconjugate Gradient (BiCG), and Biconjugate Gradient Stabilized (Bi-CGSTAB). These tend to be less robust and require more storage than CG, but they can still be very useful for solving large non-symmetric systems [19], [20]. We have implemented and tested several of these methods (see Table I) in a numerical investigation test to study the optimum and the most practical algorithm in terms of computer resources requirements, convergence and stability for the integration with the non-paraxial TD-BPM formulation. It has been observed that all the techniques used have shown good stability with a few iterations for convergence, but with different efficiency levels, as will be seen later.

IV. RESULTS AND DISCUSSIONS

In order to assess the performance of the iterative non-paraxial TD-BPM techniques rigorously, the conventional explicit FDTD was also implemented numerically for 2-D problems [4], [5]. For full understanding of the results given in this section, one has to notice the fundamental similarities and differences between the two techniques at hand. One of the main differences between the TD-BPM and the FDTD is the initial excitation of the input. This difference remains inherent to both techniques due to their different principal formulations. First the TD-BPM considers the complete input pulse profile (transverse spatial and time) right at $z = 0$, while the excitation of the input for the FDTD requires special techniques. In the following analysis, hard source technique at the edge of the computational window ($z = 0$) has been used [4]–[6]. This requires the input pulse to enter gradually from $z = 0$ and then propagates toward the positive z direction. This difference between the two initial excitations creates a concern in the assessment of the following results. Another important observation in the subsequent comparative results that should be noted is the extraction of the envelope of the pulse from the FDTD results for comparison purposes. A computer program has been written to determine the position of the envelope of the pulse out of the oscillatory TD variation of the FDTD data. This technique adds a hidden background difference when comparing the TD-BPM and the FDTD results. Other factors to be mentioned at this point is that most of the time the two methods use different Δt's which may add errors to the exact position of the peak of the pulse and the rest of the envelope data extracted from the FDTD results. In addition, shifting the pulse envelope to match each other at the peak also contributes to the following evaluation assessment.

In this section, the non-paraxial TD-BPM has been implemented to model 2-D problems by considering initially the propagation of pulsed *TE* polarized optical beam in free space. The excited initial pulsed beam considered is of the form $\varphi(x, z = 0, \tau) = \varphi_o(x)G(\tau)$, where $G(\tau)$ is a Gaussian pulsed profile defined as $G(t) = e^{-t^2/\sigma_{\tau 0}^2}$, and $\varphi_o(x)$ is the transverse spatial profile of the pulsed beam again taken as a Gaussian spatial function. The parameter $\sigma_{\tau 0}$ is the time duration of the initial pulsed beam profile. In the first example, an initial spatial waist with $w_o = 2.0$ μm, a time pulsewidth of $\sigma_{\tau 0} = 50$ fs and a wavelength of the carrier frequency of $\lambda_c = 1.0$ μm have been considered. The pulse was propagated using the non-paraxial TD-BPM along the z direction with a Padé order of $m = 2$, a temporal time step size $\Delta t = 0.8$ fs, a propagation step size $\Delta z = 0.5$ μm and $\Delta x = 0.1$ μm. The numerical parameters used in the FDTD method are: $\Delta z = \lambda_c/80 = 0.0125$ μm, $\Delta t = \Delta z/(2c_o) = 0.02848$ fs and $\Delta x = 0.1$ μm.

Fig. 1 shows comparisons between the TD-BPM and the FDTD temporal and spatial profiles at two longitudinal distances. The figure shows the close agreement between the results of the two techniques where the two curves are indistinguishable from each other. One can observe in this simulation results that Δz and Δt used in the TD-BPM are, respectively, 40 and 28 times larger than their FDTD counterparts.

The second example used to verify the accuracy and the efficiency of the non-paraxial TD-BPM involves the propagation of pulsed optical beams in a symmetric *GaAs* slab waveguide structure that has a width of 1.0 μm. At a central wavelength of $\lambda_c = 1.55$ μm, the core refractive index is $n = 3.599255$ and $n = 3.4$ for the surrounding media. The numerical parameters used for the FDTD are: $\Delta z = \lambda_c/80 = 0.019375$ μm, $\Delta x = 0.1$ μm and $\Delta t = \Delta z/(2c_o) = 0.0323$ fs. The initial pulsed beam is formed using the spatial field of the TE_o guided mode and the temporal pulse of the Gaussian profile. The pulse

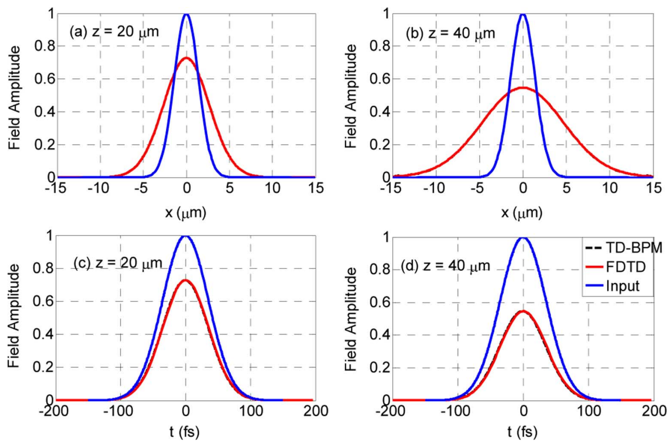

Fig. 1. Comparison between the non-paraxial TD-BPM and the FDTD results for 2-D homogenous medium implementation. Spatial profiles at (a) $z = 20\ \mu$m and (b) $z = 40\ \mu$m and temporal profiles at (c) $z = 20\ \mu$m and (d) $z = 40\ \mu$m of the propagated pulse.

field at a propagation distance of $z = 100\ \mu$m is recorded for the comparison between the two techniques. In order to fully realize the following results and due to the relatively large number of numerical parameters involved to investigate both methods, the analysis and assessment have been divided into several numerical experiments. Because it is difficult to determine the exact solution of ultra short pulse propagation in the structure described, the FDTD results were considered as references in the performance tests that follow.

To quantify the differences between the two techniques, several measuring parameters have been used. The first parameter is called the maximum percentage difference of the fields which is measured as

$$\max\langle \mathcal{M}(t)\rangle \times 100, \quad \text{for} -\frac{T}{2} \leq t \leq \frac{T}{2} \tag{7}$$

where

$$\mathcal{M}(t) = \left|E_y^B(t)\right| - \left|E_y^F(t)\right|.$$

T is the total time window and $|E_y^B(t)|$ and $|E_y^F(t)|$ are the amplitude of the fields of the TD-BPM and the FDTD, respectively, taken in the middle of the spatial window. The second parameter is the percentage root mean square (rms) difference defined as

$$\sqrt{\frac{1}{T}\int_{-T/2}^{T/2} \mathcal{M}(t)dt} \times 100, \qquad \text{for} -\frac{T}{2} \leq t \leq \frac{T}{2}. \tag{8}$$

The other two parameters used are the percentage peak difference of the pulse and the Group Velocity Ratio (GVR).

Fig. 2 shows the effect of varying the time step size Δt of the TD-BPM on the measuring parameters for the two techniques with an initial pulse duration of 100 fs. In the TD-BPM, $\Delta z = 0.1\ \mu$m and a Padé order $m = 4$ were used, while the other numerical parameters are similar to those of the FDTD. The figure illustrates that the choice of high Δt gives a high percentage differences; however the TD-BPM never become unstable. As Δt is reduced, the percentage differences decrease.

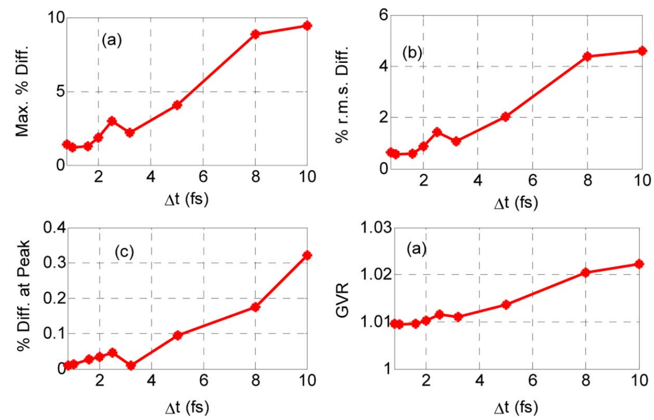

Fig. 2. The effect of varying the time step size Δt of the TD-BPM, for an initial time pulse duration of 100 fs, on (a) the percentage maximum difference, (b) the percentage root mean square of the difference, (c) the percentage difference at the peak, and (d) the Group Velocity Ratio (GVR).

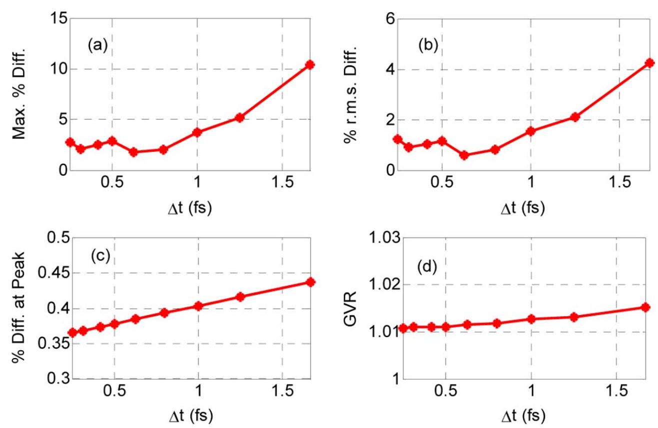

Fig. 3. The same as of Fig. 2, but with an initial pulsewidth of $\sigma_{t0} = 25$ fs.

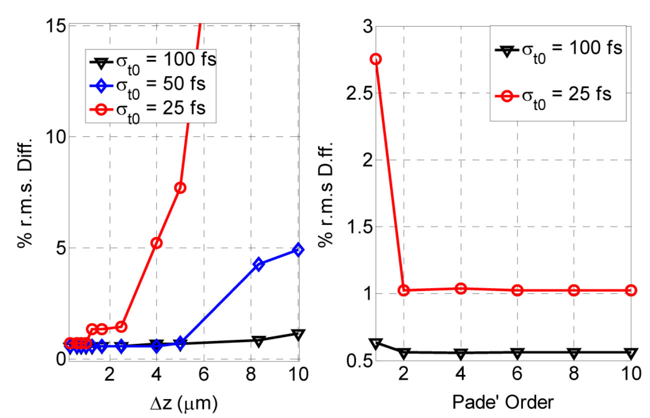

Fig. 4. Effect of varying the propagation steps size (Δz) (left) and the Pade order m (right) of the TD-BPM on the percentage "rms" difference in comparison with the FDTD for the propagation of different initial pulsed beam durations σ_{to}.

Fig. 3 shows the measuring parameters as a function of Δt for a smaller initial pulse width of $\sigma_{\tau 0} = 25$ fs. Similar observations to those of Fig. 2 can be noted. On the other hand, comparison between the two cases show that as the initial pulsewidth increases the required time steps size can be relaxed considerably. It is to be noted that the time step size of TD-BPM is around 62

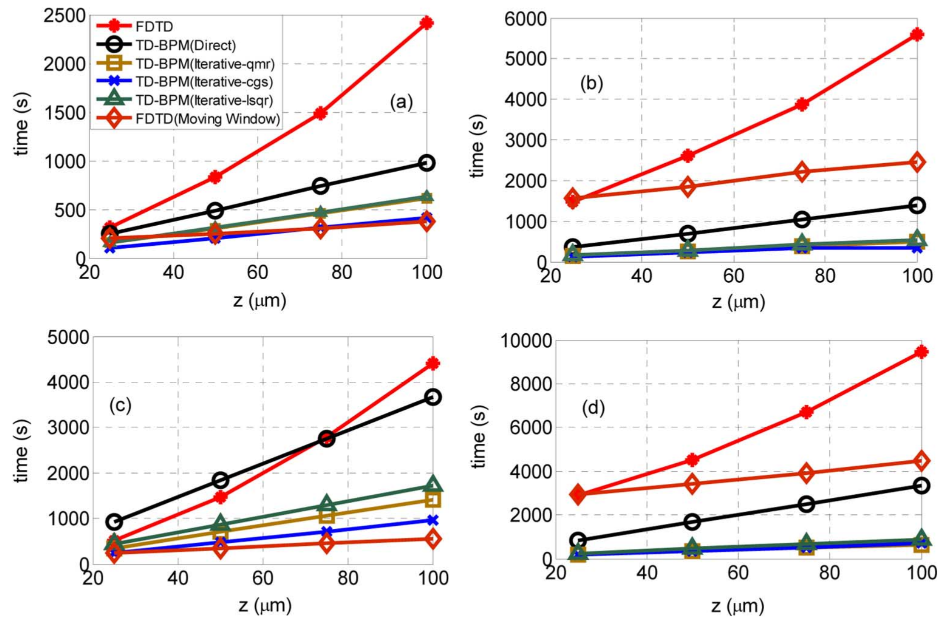

Fig. 5. Computer computational time of the FDTD and the TD-BPM using direct and different iterative techniques for 25 fs (a) and (c) and 100 fs (b) and (d) pulsed beams as a function of device length distance z for different transverse spatial step size Δx. (a) and (b) for $\Delta x = 0.1\ \mu$m; (c) and (d) for $\Delta x = 0.05\ \mu$m. Symbols: * FDTD; o TD-BPM (Direct); □ TD-BPM (iterative-qmr); × TD-BPM (iterative-cgs); △ TD-BPM (iterative-lsqr); ◊ FDTD (Moving Window).

and 23 times larger than the FDTD step size when $\sigma_{\tau 0} = 100$ fs at $\Delta t = 2$ fs and $\sigma_{\tau 0} = 25$ fs at $\Delta t = 0.75$ fs respectively, with relatively small percentage difference compared to the FDTD results.

Fig. 4 shows the effect of varying the propagation step size Δz and the Pade order m on the percentage "rms" difference between the two techniques for different initial temporal pulse widths. For the TD-BPM results, when Δz was varied in Fig. 4 (left), a Padé order $m = 4$ and time step sizes of $\Delta t = 0.4$ fs, 0.8 fs and 1.25 fs for 25 fs, 50 fs and 100 fs pulse were used respectively. Along the same line, when the Pade order m was varied in Fig. 4 (right), $\Delta z = 0.1\ \mu$m and time step size $\Delta t = 0.4$ fs and 1.25 fs for 25 fs and 100 fs pulse, respectively were used; while the other numerical parameters are similar to those of the FDTD. These numerical values were chosen such that the measuring parameters percentage difference, discussed in Figs. 2 and 3, are kept at their lowest level. Fig. 4 shows the insensitivity of changing the longitudinal step size Δz on the stability of the methods, which is a general characteristic of most implicit techniques. The figure also shows that Δz can be increased to around 100–157 times ($\Delta z = 2$–$3\ \mu$m) those of the FDTD for an initial pulse widths of $\sigma_{\tau 0} = 100$ fs and 50 fs, respectively, whereas it can be increased to 52 times of the FDTD step size for an initial pulsewidth of 25 fs ($\Delta z = 1\ \mu$m) with little change in the percentage difference. From the same figure one can also notice that the "rms" percentage difference remains relatively unchanged with the variation of the Padé order m, where a Padé order of 2 is sufficient for convergence for ultra short pulse propagation of both cases. It is also noted that the "rms" percentage difference reduces by around 0.5% whenever the temporal pulsewidth increases from 25 fs to 100 fs. It is worth to mention that an optical pulse with a 100 fs temporal width has relatively slower envelope variation in comparison with the 25 fs pulse. One may conclude from the previous analysis that the temporal step size is one of the most important numerical parameter for proper convergence of the non-paraxial TD-BPM in the case of ultra short pulse propagation. However, in this case the time step size is not directly linked to the other numerical parameters used especially the stability issue as compared with the classical FDTD.

In order to fully explore the numerical feature of the iterative TD-BPM techniques, it is also necessary to examine the numerical computational resources required along device interaction. First, Table I shows a list of the iterative methods used in the *GaAs* waveguide example described. The table shows the average number of iterations needed per propagation step for a residual of 10^{-6}. The table shows that their convergence which ranges between 2 to 4 iterations per propagation step with a maximum field difference of 10^{-4} as compared to the direct method. One feature that has been noticed is their robust stability for various numerical parameters and distances, but with variation in the total computational time. In the following analysis, only three of the most optimum iterative methods used in the TD-BPM implementations along with the direct solver have been shown.

Fig. 5 shows the total computational time of the non-paraxial TD-BPM using direct and some of the iterative techniques for 25 fs and 100 fs pulsed beams as a function of device length distance z for different transverse spatial step size Δx. A Padé order of $m = 4$, a propagation step size of $\Delta z = 0.1\ \mu$m, with time steps of $\Delta t = 1.0$ fs for $\sigma_{\tau 0} = 25$ fs and $\Delta t = 2.5$ fs for $\sigma_{\tau 0} = 100$ fs were used. The figure also shows the explicit FDTD computational time in addition to the FDTD when the spatial frame is moved with the group velocity to follow the interaction of the pulse along the z direction and it is referred to as the moving window FDTD (FDTD-MW).

For many dielectric waveguide problems, such as the one in this example, it is difficult to know the group velocity in advance. Therefore, a dynamical numerical mechanism has been

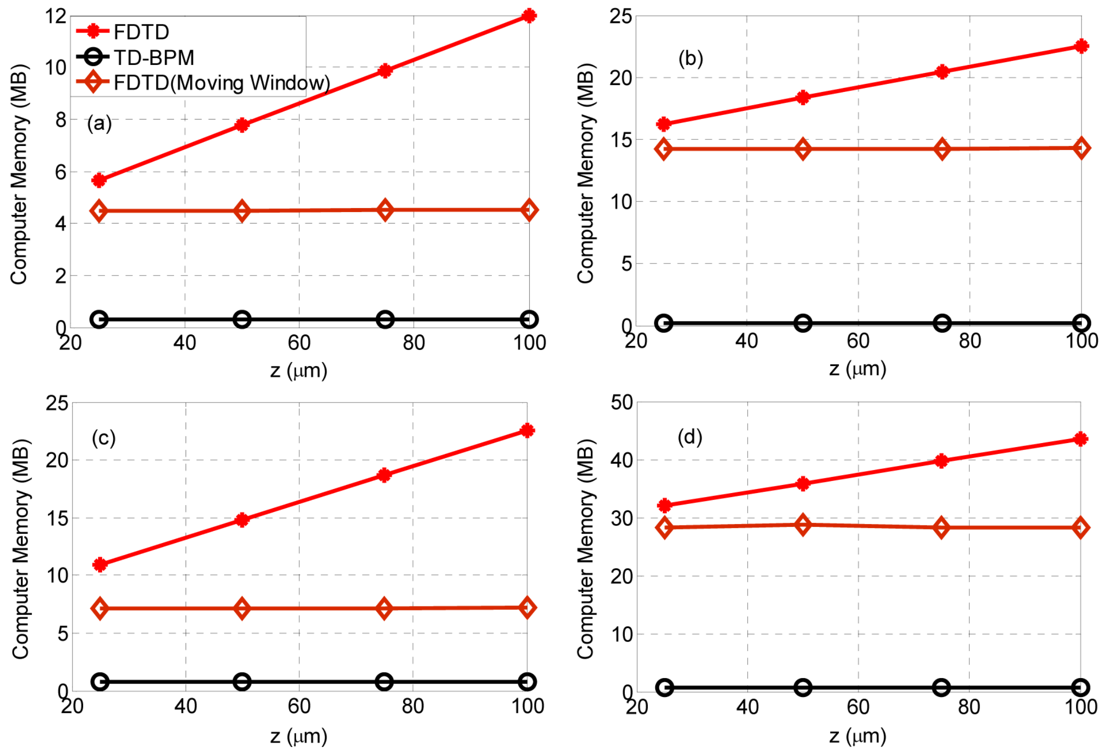

Fig. 6. Computer memory requirements for the FDTD, the TD-BPM and the FDTD-MW for 25 fs (a) and (c) and 100 fs (b) and (d) pulsed beams as a function of device length distance z for different transverse spatial step size Δx. (a) and (b) for $\Delta x = 0.1$ μm; (c) and (d) for $\Delta x = 0.05$ μm.

built to calculate the group velocity of the pulsed beam from the velocity of the pulse peak and then the spatial window was moved accordingly. This technique was also used for the movement of the time window of the TD-BPM as discussed earlier. It is worth mentioning at this point that the FDTD-MW gives frequent numerical instability when moving the spatial frame of the problem. This instability comes from the fast oscillation of the carrier frequency that makes the determination of the correct peak of the pulse a difficult task. If the group velocity cannot be determined accurately, then the movement of the spatial window becomes complicated during the course of propagation. The results for the FDTD-MW shown in Figs. 5 and 6 have been achieved after several numerical challenges using different techniques to stabilize the results, in which it was observed that these methods do not work for long device interaction. The same numerical parameters described before were used for the two FDTD techniques.

From Fig. 5, one can notice that the iterative TD-BPM techniques and the FDTD-MW generally have faster computational time compared to the classical FDTD and the direct TD-BPM for 25 fs initial pulse width. The FDTD computational time increases nonlinear with the device length, while the TD-BPM changes linearly with the device length. On the other hand, for 100 fs initial pulse width, the iterative TD-BPM techniques have similar computational time and they all have better performance with the increase of z as compared to the FDTD, the MW-FDTD and the direct TD-BPM. Fig. 6 shows the corresponding computer memory requirement of the FDTD, the FDTD-MW and the TD-BPM for 25 fs and 100 fs pulsed beams as a function of device length distance z for different transverse spatial step size Δx. It is to be mentioned that the direct and the iterative TD-BPM techniques discussed require almost the same computer memory space. The figure shows that memory requirement by the FDTD increases linearly with the size of the device, while it remains constant in the case of the TD-BPM and the FDTD-MW due to the moving window concept. In addition and despite the stability problem of the FDTD-MW discussed, comparison between the TD-BPM and the FDTD-MW in terms of computer memory requirements shows that the TD-BPM is always much better as compared to the FDTD-MW. For example, the FDTD-MW requires around 14 and 68 times more computer memory than the TD-BPM for $\sigma_{t0} = 25$ fs and $\sigma_{t0} = 100$ fs, respectively, for the case of $\Delta x = 0.1$ μm. While, for example at z $= 100$ μm, the FDTD consumes around 38 and 107 times more computer memory than the TD-BPM for $\sigma_{t0} = 25$ fs and $\sigma_{t0} = 100$ fs, respectively, for the case of $\Delta x = 0.1$ μm.

Finally, all above implementations were performed using an Intel core i5 750 with 2.67 GHz Processor.

V. Conclusion

In this work, the non-paraxial Time Domain Beam Propagation Method (TD-BPM) to model ultra short pulse propagation in dielectric waveguides using a number of iterative numerical techniques have been implemented and analyzed. The method relies on unidirectional pulse propagation that allows the time window to move and follow the interaction of pulses along the direction of propagation. The Pade approximant has been used effectively to overcome the paraxial limit for ultra short pulse durations. The method was tested rigorously along with the classical FDTD. It was observed that the iterative TD-BPM techniques are very stable and accurate. Both the longitudinal and the temporal steps sizes can be a number of orders of magnitude larger than the FDTD step sizes. Computer performance tests showed that the TD-BPM is more efficient than the FDTD in terms of computer time and memory requirements for unidirectional long device interaction. In addition, the moving window FDTD-MW has been implemented for efficiency comparison purposes by moving the spatial coordinate of the FDTD. Comparison between the TD-BPM and the FDTD-MW showed that the TD-BPM has much better usage of computer memory. It was found that it is difficult to implement the FDTD-MW due to the numerical instability in determining the exact group velocity which is necessary to move the spatial window dynamically. Therefore, it is concluded that the iterative TD-BPM is efficient in the analysis of short and ultra short pulse propagation in long device structures.

References

[1] P. Vasa, C. Ropers, R. Pomraenke, and C. Lieau, "Ultra-fast nano-optics," *Laser & Photon Rev.*, vol. 3, no. 6, pp. 483–507, 2009.
[2] G. Steinmeyer, "A review of ultrafast optics and optoelectronics: Review article," *J. Opt. Aperture Appl. Opt.*, vol. 5, pp. R1–R15, 2003.
[3] K. S. Yee, "Numerical solution of initial boundary value problems involving Maxwell's equations in isotropic media," *IEEE Trans. Antennas Propag.*, vol. AP-14, no. 5, pp. 302–307, May 1966.
[4] A. Taflove and S. C. Hagness, *Computational Electrodynamics: The Finite-Difference Time-Domain Method*. Norwood, MA: Artech, 2000.
[5] D. M. Sullivan, *Electromagnetic Simulation Using the FDTD Method*, 1st ed. New York: Wiley-IEEE Press, 2000.
[6] R. Mittra, Y. Liu, X. Yang, and Y. Wenhua, *Electromagnetic Simulation Techniques Based on the FDTD Method*. New York: Wiley, 2009.
[7] S. Ju, K. Jung, and H. Kim, "Investigation on the characteristics of the envelope FDTD based on the alternating direction implicit scheme," *IEEE Microw. Wireless Compon. Lett.*, vol. 13, no. 9, pp. 414–416, Sep. 200.
[8] H. Rao, R. Scarmozzino, and R. M. Osgood, "An improved ADI-FDTD method and its application to photonic simulations," *IEEE Photon. Technol. Lett.*, vol. 14, no. 4, pp. 477–479, Apr. 2002.
[9] S. G. García, T. W. Lee, and S. C. Hagness, "On the accuracy of the ADI-FDTD method," *IEEE Antennas Wireless Propag. Lett.*, vol. 1, pp. 31–34, 2002.
[10] Q. Liu, Z. Chen, and W. Yin, "An arbitrary-order LOD-FDTD method and its stability and numerical dispersion," *IEEE Trans. Antennas Propag.*, vol. 57, no. 8, pp. 2409–2417, Aug. 2009.
[11] F. Zheng and Z. Chen, "Numerical dispersion analysis of the unconditionally stable 3-D ADI-FDTD method," *IEEE Trans. Microw. Theory Tech.*, vol. 49, no. 5, pp. 1006–1009, May 2001.
[12] J. Shibayama, A. Nomura, R. Ando, J. Yamauchi, and H. Nakano, "A frequency dependent LOD-FDTD Method and its application to the analyses of plasmonic waveguide devices," *IEEE J. Quantum Electron.*, vol. 46, no. 1, pp. 40–49, Jan. 2010.
[13] K. Y. Jung, F. L. Teixeira, S. G. Garcia, and R. Lee, "On numerical artifacts of the complex envelope ADI-FDTD method," *IEEE Trans. Antennas Propag.*, vol. 57, no. 2, pp. 491–498, Feb. 2009.
[14] J. Shibayama, M. Muraki, R. Takahashi, J. Yamauchi, and H. Nakano, "Performance evaluation of several implicit FDTD methods for optical waveguide analysis," *J. Lightw. Technol.*, vol. 24, no. 6, pp. 2465–2471, Sep. 2006.
[15] J. N. Shibayama, M. Muraki, J. Yamauchi, and H. Nakano, "Comparative study of several time-domain methods for optical waveguide analyses," *J. Lightw. Technol.*, vol. 23, no. 7, pp. 2285–2293, Jul. 2005.
[16] H. M. Masoudi, M. A. AlSunaidi, and J. M. Arnold, "Time-domain finite-difference beam propagation method," *IEEE Photon. Technol. Lett.*, vol. 11, no. 10, pp. 1274–1276, Oct. 1999.
[17] H. M. Masoudi, M. A. AlSunaidi, and J. M. Arnold, "Efficient time-domain beam propagation method for modeling integrated optical devices," *J. Lightw. Technol.*, vol. 19, no. 5, pp. 759–771, May 2001.
[18] H. M. Masoudi, "A novel nonparaxial time-domain beam-propagation method for modeling ultrashort pulses in optical structures," *J. Lightw. Technol*, vol. 25, no. 10, pp. 3174–3185, Oct. 2007.
[19] R. Barrett, M. Berry, T. F. Chan, J. Demmel, J. Donato, J. Dongarra, V. Eijkhout, R. Pozo, C. Romine, and H. Van der Vorst, *Templates for the Solution of Linear Systems: Building Blocks for Iterative Methods*, 2nd ed. Philadelphia, PA: SIAM, 1994.
[20] Y. Saad, *Iterative Methods for Sparse Linear Systems*, 2nd ed. Philadelphia, PA: SIAM, 2003.
[21] F. A. Milinazzo, C. A. Zala, and G. H. Brooke, "Rational square-root approximations for parabolic equation algorithms," *J. Acoust. Soc. Amer.*, vol. 101, pp. 760–766, Feb. 1997.
[22] D. Yevick and D. J. Thomson, "Complex Padé approximants for wide-angle acoustic propagators," *J. Acoust. Soc. Amer.*, vol. 108, no. 6, pp. 2784–2790, 2000.
[23] H. Rao, M. J. Steel, R. Scarmozzino, and R. M. Osgood, Jr., "Complex propagators for evanescent waves in bidirectional beam propagation method," *J. Lightw. Technol.*, vol. 18, no. 8, pp. 1155–1160, Aug. 2000.
[24] M. D. Collins, "Applications and time-domain solution of higher-order parabolic equations in underwater acoustics," *J. Acoust. Soc. Amer.*, vol. 86, no. 3, pp. 1097–1102, Sep. 1989.

Husain M. Masoudi received the B.S. and M.S. degrees in electrical engineering from King Fahd University of Petroleum and Minerals (KFUPM), Dhahran, Saudi Arabia, in 1986 and 1989, respectively, and the Ph.D. degree in electronics and electrical engineering from the University of Glasgow, Glasgow, U.K., in1995.

He was promoted to Assistant Professor, Associate Professor, and Professor, respectively, in 1995, 2002, and 2011, in the Department of Electrical Engineering at KFUPM. From 1998 to 2004, he was a Manager of Laser Research Section, Center for Applied Physical Sciences, Research Institute, KFUPM. He was a Visiting Research Professor to several research labs and departments such as the Emerging Communications Technology Institute at the University of Toronto, Toronto, ON, Canada, during 2006–2007, the Institute of Chemical Process Fundamentals, the Czech Academy of Sciences, Prague, Czech Republic in 2003, the Electrical and Electronic Engineering Department, Imperial College of Science, Technology and Medicine, London, U.K., in 2001, the Electronics and Electrical Engineering Department, University of Glasgow in 1996 and 1998. His academic research interest includes electromagnetic field interactions with linear and nonlinear materials, optical fiber communications and lasers and their applications. His current research interest is modeling linear and nonlinear optical devices. This includes CW interactions and pulsed optical beams.

Mohammad S. Akond, biography not available at the time of publication.